

Transition Region Blinkers: II Active-Region Properties

C.E. Parnell (clare@mcs.st-and.ac.uk) and D. Bewsher
*Mathematical Institute, University of St Andrews, North Haugh, St Andrews,
KY16 9SS*

R.A. Harrison
*Space Science Department, Rutherford Appleton Laboratory, Chilton, Didcot,
Oxfordshire, OX11 0QX*

Abstract. The distribution and general properties of events identified in an active region that have the same characteristics as quiet-Sun blinkers are discussed and named ‘active-region blinkers’. The events are identified using an automated scheme ‘Blinker Identification Program’ (BLIP) which was designed for and tested on quiet-Sun blinkers. Like quiet-Sun blinkers, the active-region events are most easily identified in the 629 Å emission line from O V although evidence for them is also found in other extreme UV lines emitted from He I, O III and O IV. Unlike quiet-Sun blinkers, however, they may also have coronal signatures in the lines Mg IX and Mg X. Their properties are very similar to those of quiet-Sun blinkers with mean lifetimes of 16 – 19 minutes, mean areas of $2.4 - 4.3 \times 10^7$ km² and mean intensity enhancements factors of 1.8 – 3.3. Their global frequency of $7 - 28$ s⁻¹ is about 42% – 700% higher than that for quiet-Sun blinkers. The blinkers discussed here are found above both active-region (plage) magnetic fields, as well as above the umbra and penumbra of a sunspot.

1. Introduction

A number of authors including Harrison (1997), Berghmans et al. (1998), Harrison et al. (1999), Brković et al. (2001) and more recently Bewsher et al. (2001) (here after Paper 1) have reported on blinkers identified in transition region lines in quiet-Sun regions. Blinkers are small-scale intensity enhancements in the transition region that can be observed best in the 629 Å emission line from O V which forms at 2.5×10^5 K, but can also be found in other extreme UV (EUV) lines with temperatures down to 2×10^4 K. It is possible that quiet-Sun blinkers (QS blinkers) may occur at higher temperatures. The Mg IX (368 Å) and Mg X (624 Å) lines which form at 10^6 K and 1.2×10^6 K, respectively, only show faint enhancements at the same time as a QS blinker is observed in O V. Recently, a comprehensive survey of several hundred QS blinkers has been carried out (Paper 1) and the results confirm that blinkers have the following properties: (i) mean area of 3×10^7 km²; (ii) mean lifetime of 16 minutes; (iii) a typical intensity enhancement factor of 1.8; and (iv) a global frequency of between 1 s⁻¹ and 20 s⁻¹. They are not temperature events, but density enhancements or increases in filling



© 2001 Kluwer Academic Publishers. Printed in the Netherlands.

factor. They are mostly found over regions of enhanced chromospheric or transition region emission such as network boundaries and seem to preferentially occur above regions of strong magnetic fields where one polarity dominates. Furthermore, Fourier and wavelet analyses do not reveal any periodic behavioural patterns in the light curves of the blinkers despite the apparent appearance of reoccurring blinking in them.

Blinkers have until now been considered inherently a quiet-Sun phenomena, however, there is some evidence that blinker-type events may also occur in active regions. For instance, using the Harvard EUV Spectrometer on Skylab, Withbroe et al. (1985) report that frequent localized short-term fluctuations were observed in chromospheric, transition region and coronal lines. Approximately 20% of the $5'' \times 5''$ pixels had intensity variations exceeding a factor of 1.3 for the H I $L\alpha$ (1216 Å) which has a formation temperature of $\approx 2 \times 10^4$ K, a factor of 1.5 for the C III (977 Å), O IV (554 Å) and O VI (1032 Å) lines which are formed at mean temperatures of 10^5 , 2×10^5 and 3×10^5 K and a factor of 1.4 for the Mg X (625 Å) line which is formed at about 2×10^6 K. The pixels on the Skylab Spectrograph are a factor 3.5 larger than those on Coronal Diagnostic Spectrometer on SOHO and the cadence of the data used by Withbroe et al. (1985) was just 5.5 minutes. However, they find that significant variations in these EUV lines occur over temporal intervals of 5 to 15 minutes and with spatial scales of $5''$ to $15''$. A number of other authors (cf. Lites and Hansen, 1977; Bruner and Lites, 1979; Athay et al., 1980; Dere et al., 1981; Athay, 1984; Porter et al., 1984 and Habbal et al., 1985) report observations of UV ‘bursts’ or impulsive variations in emission from spectral lines formed in the lower transition region ($T \approx 10^5$ K) in active regions using data from OSO-8, HRTS and SMM and the Harvard Spectrograph on Skylab. The ‘bursts’ were found to be a common, nearly continuous phenomena, in active regions. More recently, Walsh et al. (1997) studied a set of high cadence (14 seconds) CDS data including the He I (584 Å) chromospheric line, the O V (629 Å) transition region line and the Mg IX (368 Å) and Fe XVI (360 Å) coronal lines. They identified two events that seemed to fit the description of a blinker, and, hence, named them ‘active-region blinkers’ (AR blinkers). These events showed signatures at all four wavelengths. They had length scales of 14 and 18 Mm, lifetimes of 10 and 16.5 minutes and intensity enhancements of 2.5 and 4. Due to the high cadence of their data, Walsh et al. (1997) were able to determine that the signatures in O V occurred before the start of the events in He I and the events in both Mg IX and Fe XVI. This result suggests that these events are neither heating nor cooling and is consistent with the findings for QS blinkers which are believed not

to be temperature events. Doppler velocities of between 30 and 70 km s⁻¹ were observed and a positive correlation between the line width and Doppler velocity were also found suggesting that they are not unidirectional. The location of the events above the magnetic field was discussed with one event found above a region of positive magnetic field whilst the other appear over negative magnetic field.

These observational results are highly suggestive that blinkers may also occur in active regions. Furthermore, from our observations of QS blinkers (Paper 1) there do not appear to be any physical reasons why blinkers could not occur in active regions. Blinkers are simply enhancements in emission from chromospheric and transition region EUV lines and are seen best in emission lines with temperatures of formations around 10⁵ to a few times 10⁵ K, (e.g., O V 629 Å and O IV 554Å). From ratios of oxygen emission lines they do not appear to be temperature events, however, this may simply be due to the low temporal resolution of data sets analysed so far. They are general seen above areas of enhanced network which also occur in active regions and so it seems logical that they may also be found in active regions. The aim of this paper is, therefore, to look for blinker-type events in active regions and to characterise any events we find to determine if they are the same as QS blinker. Firstly, the active-region data set is described as are the methods used to analyse the data and detect the events (Section 2). In Section 3, the characteristics of the events found are presented and compared with the QS blinkers of Paper 1. We also investigate the relationship of the events found in O V with emission from the chromospheric and coronal lines. Finally, the conclusions are given in Section 4 including a discussion of the connection between our events and other active-region phenomena.

2. Data and Analysis

The data used in this paper was taken with the Coronal Diagnostic Spectrometer (CDS; Harrison et al., 1995) and the Michelson Doppler Imager (MDI; Scherrer et al., 1995) instruments, both aboard the Solar and Heliospheric Observatory (SOHO).

Normal incidence spectrometer (NIS) data from CDS (CDS run numbers S11478 and S11479) are analysed in this paper. The data was taken using the CDS BLINK_ST sequence and contains 6 EUV emission lines: He I (584 Å), O III (599 Å), O IV (554 Å), O V (629 Å), Mg IX (368 Å) and Mg X (624 Å). These lines are representative of plasma temperatures of 2 × 10⁴ K, 10⁵ K, 1.6 × 10⁵ K, 2.5 × 10⁵ K, 10⁶ K and 1.2 × 10⁶ K, respectively. The data sequences consist of

rasters that cover an area $40'' \times 124''$ (10×73 pixels), with each pixel sized $4'' \times 1.6''$. The exposure time at each slit location is just 10 seconds making the cadence of the entire raster approximately 151 seconds.

The S11478 data sequence started on 18th June 1998 at 18:17 UT. It was immediately followed by the S11479 data set. Both data sets are feature tracking with the use of the internal mirror and then, once the mirror has reached its maximum offset, by the movement of the legs. They were joined together to make one data set which lasted 6 hours. A segment of a high resolution MDI image the same size as the CDS rasters can be seen on the right-hand side of Figure 1 and shows the magnetic field below the CDS data. Its position on the Sun is indicated by a small white rectangle in the full disc MDI image on the left-hand side of Figure 1. It is clear that the region observed lies above an active region and contains a large positive polarity sunspot that dominates the field of view. The coordinates of the first raster are $39.6''$ E and $295.7''$ N.

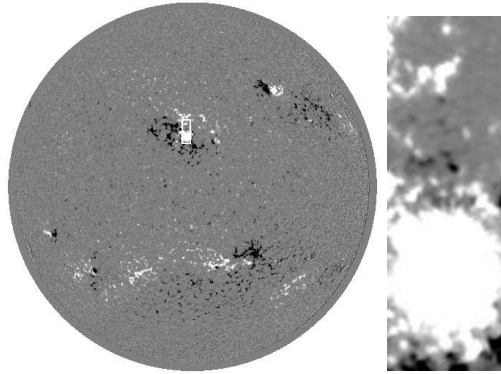


Figure 1. Full disk MDI magnetogram (left) taken on 18th June 1998 at 19:12 UT. The small white rectangle indicates the area covered by the CDS rasters investigated. Partial frame high resolution MDI magnetogram (right) taken 5 minutes earlier showing the magnetic field below the CDS rasters.

The standard CDS procedures are used to correct for missing pixels, CCD readout bias and cosmic ray hits and flat fielding effects. The data units are also changed to photons per pixel per second (p/p/s) using a standard calibration. The only non standard procedure used in the preparation of the data is that used for correcting the tilt between the NIS dispersion axis and the CCD detector (Bewsher et al., 2002). The CDS procedure ROTXY from solarsoft (a suite of IDL routines for analysis of data, e.g., from Yohkoh and SOHO) is used to remove the effect of solar rotation, and bi-linear interpolation is used to account for any sub pixel rotation.

The MDI data used is from the high resolution field of view and has a cadence of 1 minute and a pixel size of $0.6'' \times 0.6''$. The MDI images are grouped and averaged to reduce the cadence to that of the CDS data. This technique also reduces the noise in the MDI data. The pointing information in the headers of the CDS and MDI data were used for alignment purposes. An inspection by eye suggests that a good alignment is achieved.

In order to objectively detect blinkers from a series of SOHO/CDS rastered images we use the automated BLinker Identification Program (BLIP). Full details of BLIP can be found in Paper I. The algorithm finds groups of pixels that have ‘significant’ simultaneous temporal peaks and classifies them as a blinker. First all the pixels are considered separately and the temporal local maxima and minima in each pixel are identified. Not all of these maxima are going to be associated with a blinker. We define a ‘significant’ peak to be a peak that has an intensity $n_\lambda \lambda$ greater than the troughs immediately before and immediately after it, where λ is defined as the value below which 99% of the errors exist and n_λ is a parameter that typically takes the value 3, 5 or 10. Once we have identified all the ‘significant’ peaks in the individual pixels we look for adjacent pixels that simultaneously have ‘significant’ peaks. To be a blinker there must be at least n_p pixels that peak simultaneously in each group. The parameter, n_p , is typically taken to be either 1,2, or 3 CDS pixels. Finally, when each group of pixels is identified we once more check the intensity light curve of the group and make sure that it still produces a significant peak at the same time as the individual pixels that make up the group peaked. The physical properties of the blinkers are also identified.

3. Results

3.1. BLINKER PROPERTIES

We use BLIP to investigate a series of different sizes of events by varying the minimum size, n_p , and the minimum intensity factor, n_λ , in each run of our algorithm. The error threshold, λ , of the O V data equals 6.97 photons per pixel per second (p/p/s). Table I shows the numbers and properties of blinkers identified in O V.

From Table I it is clear that the properties of the O V events identified by BLIP in the active region have similar properties to QS blinkers, as discussed in the Introduction and presented in Paper 1, and so we call these events active-region blinkers (AR blinkers). Note, however, until we have considered their line ratios (which we do in section 3.3) we cannot say for certain that they really are blinkers.

Table I. Properties of O V active-region events identified using BLIP.

Properties	n_λ	3	5	5	5	10
	n_p	3	1	2	3	3
No. of blinkers		253	224	163	125	64
Global frequency (s^{-1})		27.7	24.5	17.8	13.7	7.0
Mean intensity enhancement factor		1.8	2.1	2.2	2.4	3.3
Mean area ($\times 10^7 \text{ km}^2$)		3.3	2.4	3.2	3.9	4.3
Mean lifetime (minutes)		16.5	18.0	17.7	17.5	19.3
Mean rise time (minutes)		8.2	8.8	8.5	8.6	9.5
Mean fall time (minutes)		8.3	9.3	9.2	8.9	9.8

The mean lifetimes and mean areas of the O V AR blinkers are slightly longer and larger than those found in Paper 1 for the QS blinkers. Indeed, for each parameter set the mean lifetimes of the AR blinkers are at most 10% longer than for the QS blinkers, whilst their areas are between 6% and 50% larger. The lifetimes of the AR blinkers are similar to those observed by Walsh et al. (1997) for their two blinker-like events. As one would expect an increase in n_λ generally leads to an increase in both the area and lifetime of the blinkers as the smaller, weaker events are discounted, however, as n_p increases the mean areas increase, but the mean lifetimes fall. The largest blinker observed has an area of $2.7 \times 10^8 \text{ km}^2$ (75 pixels) and covers just over 10% of the raster area. The minimum area of a blinker is, of course, restricted by the choice of n_p and equals $3.6n_p \times 10^6 \text{ km}^2$. The longest lived blinker lasts for just under 42 minutes and is a $n_\lambda = 3$ and $n_p = 3$ blinker. The minimum lifetime of the blinkers is just over 5 mins which is restricted by the time resolution of the data.

The mean rise and fall times of the AR blinkers are consistent with those for the QS blinkers as they again appear to be approximately equal (if anything the mean fall time is slightly longer than the mean rise time). However, if the individual blinkers are considered it is found that about 40% have longer rise times than fall times, similarly about 40%, have the reverse and only 20% have rise times approximately equal to their fall times. This variation in rise and fall times is consistent with the two events found by Walsh et al. (1997) where it was found that one event had a rise time greater than fall time whilst the other had a rise time less than its fall time.

Just like the mean areas of the blinkers their mean intensity enhancement factors are between 6% and 57% larger than those for the

QS blinkers. Furthermore, they also increase with increasing n_λ and n_p . It is important to note that the values of λ in the active region are considerably larger than those in the quiet Sun, hence the actual sizes of the intensity enhancements here are larger still than those in the QS blinkers.

Once again the active region lives up to its name and is found to be more ‘active’ than the quiet Sun, since it produces blinkers more frequently. Indeed, the global frequencies show that at least 42% more blinkers occur in an active region than in the quiet Sun. The choice of parameters clearly varies the number of blinkers identified. Decreasing the value of n_p from 3 to 2, and from 2 to 1 produces 37% and 30% more blinkers, respectively. A bigger increase is caused, however, with the reduction of n_λ from 10 to 5 and 5 to 3 where the number of blinkers identified is practically doubled in each case. These increases are similar to those found for the QS blinkers in Paper 1.

3.2. SIGNATURES OF ACTIVE REGION BLINKERS

Figure 2 shows the light curves of a typical AR O V blinker in six different wavelengths (He I, O III, O IV, O V, Mg IX and Mg X). The O V light curve of the blinker is very similar to those observed for QS blinkers (Paper 1). This blinker was detected using the O V wavelength, however, it is also clearly detectable in all other wavelengths other than Mg IX. In the Mg IX we do see an event, but it’s peak is not significant enough to be counted as a blinker. If we calculate the difference between the peak intensity and maximum of the two troughs either side of the peak we find that the event has a jump equal to $n_{\lambda MgIX} \lambda_{MgIX}$, where $n_{\lambda MgIX}$, the peak factor is just 3.7 as opposed to 5, the value of n_λ . Indeed, if we calculate all the peak factors in the different wavelengths for this blinker we find they equal 31, 8.8, 20, 23 and 6.4 for He I, O III, O IV, O V and Mg X, respectively. Clearly, this blinker is a strong event yet, its signature is only just identified in O III and Mg X. This is probably a reflection of the strength of these lines rather than a significant feature of the blinkers.

We have analysed the O V blinkers to determine how many register as blinkers in the other wavelengths observed. The results are shown in Table II. For all values of n_λ and n_p at least 67-82% of blinkers seen in O V can also be identified in O IV, 59-73% in He I and 16-28% in O III. As in the quiet-Sun case, all the blinkers seen in O III are also visible in O IV and He I. In Mg IX, 6-10% of OV blinkers are seen, whereas in the Mg X, 11-18% are identified. All except one of the Mg IX blinkers can be readily identified in all the other wavelengths, whilst

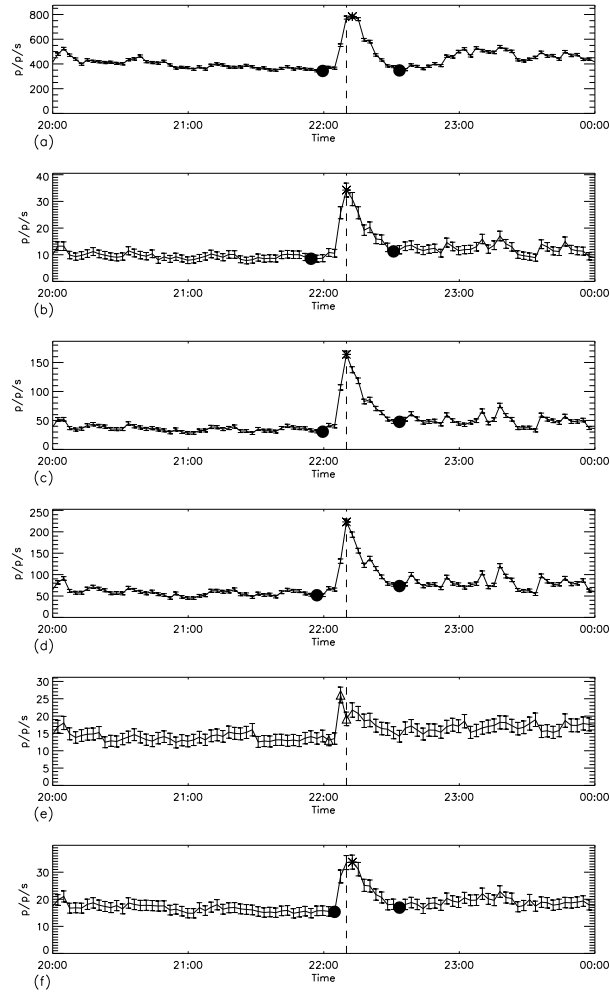


Figure 2. Comparison of light curves for a blinker identified in O V and seen in different wavelengths: (a) He I; (b) O III; (c) O IV; (d) O V; (e) Mg IX and (f) Mg X. The stars mark the peaks identified as blinkers and the dots mark their starts and ends whilst the triangles mark the start, peak and end of any event not counted as a blinker. The dashed line indicates time of the peak of the O V blinker.

all except two of Mg X blinkers are detected as blinkers in He I, O III, O IV, and O V.

Even though in some emission lines, in particular Mg IX and Mg X, a blinker is not always detected a peak signature is often seen. We calculate the peak factors of all the signatures that occur simultaneously with the blinkers identified in O V to determine the strengths of the events seen. Table III gives the λ values for each wavelength, as well as the minimum and maximum peak factors observed. We find that in all

Table II. Numbers of blinkers identified in O V and other wavelengths.

Wavelength	n_λ	3	5	5	5	10
	n_p	3	1	2	3	3
O V		253	224	163	125	64
He I/O V		158	133	105	85	47
O III/O V		68	35	32	30	18
O IV/O V		194	149	117	102	49
Mg IX/O V		19	13	12	12	4
Mg X/O V		30	25	23	22	10
He I/O III/O V		64	35	32	30	18
He I/O IV/O V		143	120	95	83	41
He I/Mg IX/O V		19	13	12	12	4
He I/Mg X/O V		29	25	23	22	10
O III/O IV/O V		68	35	32	30	18
O III/Mg IX/O V		19	12	12	12	4
O III/Mg X/O V		29	24	22	21	10
O IV/Mg IX/O V		19	13	12	12	4
O IV/Mg X/O V		30	25	23	22	10
Mg IX/Mg X/O V		19	12	12	12	4
He I/O III/O IV/O V		64	35	32	30	18
He I/O IV/Mg IX/O V		19	13	12	12	4
He I/O IV/Mg X/O V		29	25	23	22	10
O III/O IV/Mg IX/O V		19	12	12	12	4
O III/O IV/Mg X/O V		29	24	22	21	10
O IV/Mg IX/Mg X/O V		19	12	12	12	4
He I/O III/O IV/Mg IX/O V		19	12	12	12	4
He I/O III/O IV/Mg X/O V		28	24	22	21	10
O III/O IV/Mg IX/Mg X/O V		19	12	12	12	4
He I/O III/O IV/Mg IX/Mg X/O V		19	12	12	12	4

wavelengths 47% of the O V blinkers have peak factors greater than 1 whilst 15% have peak factors greater than 3. The minimum peak size factor of 0.0 in the He I, Mg IX and Mg IX lines indicate that there is not always an event identified in these wavelengths. However, all maximum peak factors are well over the $n_\lambda = 5$ criteria, implying that all wavelengths have a high enough intensity and sufficient variability

Table III. Range of peak factors for events in all wavelengths associated with blinkers identified in O V with $n_\lambda = 5$ and $n_p = 3$.

Wavelength	λ	Minimum peak factor	Maximum peak factor	% w. peak factor > 1	% w. peak factor > 3
He I	14.11	0.0	115.4	92.0	78.4
O III	2.78	0.1	32.7	89.6	52.0
O IV	6.26	1.7	66.3	100.0	93.6
O V	6.97	5.3	82.8	100.0	100.0
Mg IX	2.72	0.0	15.2	47.2	15.2
Mg X	2.73	0.0	21.9	71.2	24.0

to identify the blinkers. Therefore, the absence of any signature of an event in the helium or magnesium lines is probably real and suggests that blinkers are likely to be caused by something that happens in the transition region, rather than blinkers being the transition regions response to events in either the chromosphere or corona.

3.3. LINE RATIOS

It has been well established (Harrison et al., 1999, Paper 1) that the intensity increases of QS blinkers are due to enhancements in either density or filling factor rather than temperature. Clearly, this fact also needs to be established for the blinkers seen in active regions to check they really are the same type of phenomenon. To do this we look at the line ratios of the oxygen light curves.

Figure 3a shows the light curve of the O V blinker seen in Figure 2d. The line ratios of the O V line with the He I, O III and O IV lines are also shown in Figure 3b-d, respectively. The dashed line marks the time of the peak of the O V blinker. In this case, it appears as if the line ratios of the oxygen species dip around the time of the blinker, although the dips are only slight and within the error bars. If these dips are real then it would imply that active-region blinkers are slightly cooler events than their surroundings.

To determine the significance of these dips and to test whether these dips are a common feature in AR blinkers we investigate the variability of the line ratios. We do this by calculating the minimum, mean and maximum values of the light curves between the start and end of the blinker and also over the entire light curve (Table IV). If the differences between the entire light curve ratio and blinker light curve ratio values

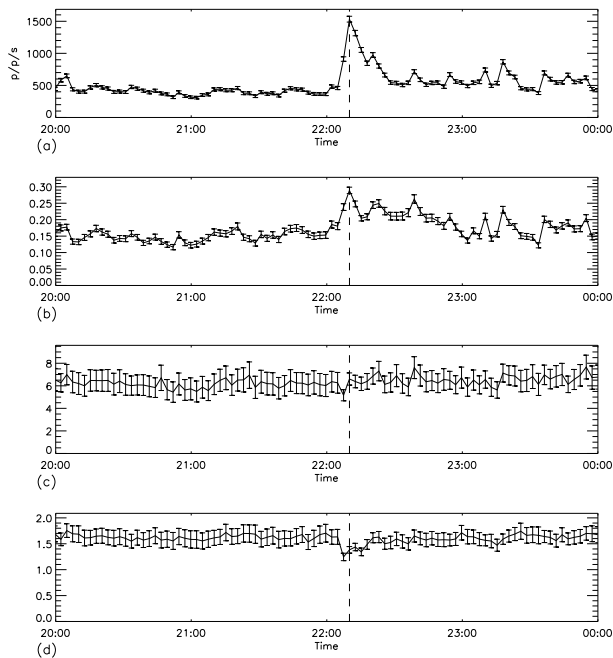


Figure 3. (a) O V blinker light curve, (b) O V/He I line ratio, (c) O V/O III line ratio and (d) O V/O IV line ratio. The dashed line indicates the peak of the O V blinker.

Table IV. Minimum, mean and maximum line ratio values for the entire light curve and for the blinker region only.

Wavelength	Minimum		Mean		Maximum	
	Entire	Blinker	Entire	Blinker	Entire	Blinker
O V/O III	3.74	3.60	8.37	8.77	36.88	39.24
O V/O IV	1.16	1.09	1.66	1.64	3.68	3.67

are larger than the typical error bars expected then the change is considered significant. From the results in Table IV it appears as if there is little variation in the oxygen species between the entire and the blinker light curve ratios, even though the maximum, mean and minimum values are themselves quiet different. The typical errors on the ratios of the O V/O III and O V/O IV are 1.32 and 0.14, respectively, however, the difference between the entire and blinker line ratios are always less than these errors except in the case of the maximum line ratio values for O V/O IV. We, therefore, conclude that these ratios are

again effectively flat and thus AR blinkers are enhancements in either density or filling factor just like the QS blinkers.

3.4. RELATIONSHIP TO ACTIVE REGION EMISSION

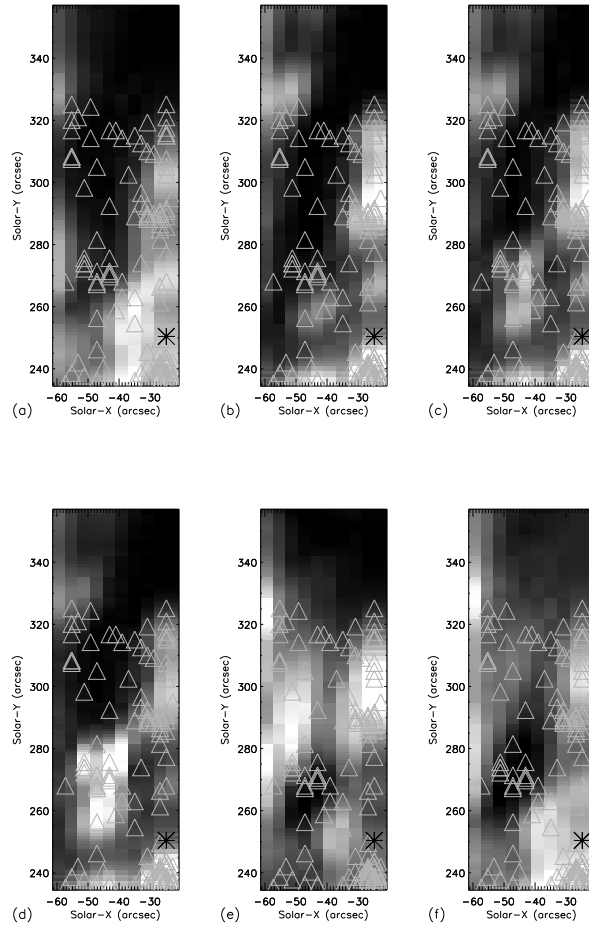


Figure 4. Comparison of the location of blinkers with the active-region network. Time integrated emission of the derotated (a) He I, (b) O III, (c) O IV, (d) O IV, (e) Mg IX and (f) Mg X rasters. Each Δ identifies the location of a blinker and the * refers to the blinker shown in Figure 2d.

It has been found that QS blinkers preferentially occur above quiet-Sun network regions. Indeed, in Paper 1 it was found that no QS blinkers occurred in the bottom 5-10% of the intensity range in He I, O III, O IV, and O IV. However, the same result is not true for the

coronal lines where QS blinkers were found at all intensity levels. It is interesting to test to see if this is still the case for AR blinkers.

Figure 4 shows the emission integrated over time from each of the six CDS wavelengths, with the location of the blinker midpoints plotted as Δ s. The * marks the blinker seen in Figure 2d. Clearly, the spatial distribution of the blinkers is not uniform, however, as in the QS case, we test to see if the distribution of blinkers with respect to intensity in the different wavelengths is uniform. To do this we use a likelihood statistical test (as in Paper I). We determine the numbers of pixels with intensities in certain ranges (bins), of which there are k , and are chosen such that the width of the bins increase by a factor of 2 for increasing intensity. We define M to be the total number of pixels and M_i to represent the numbers of pixels in the i th range. Similarly, n represents the total number of pixels associated with the peak of each blinker whilst n_i is the number of these pixels with intensities in the i th range. The likelihood ratio statistic, w_k , is then defined as

$$w_k = 2n_i \sum_{i=1}^k \log \left(\frac{n_i M}{n M_i} \right), \quad (1)$$

and is compared with the expected χ_{k-1}^2 statistic. If w_k is large compared to χ_{k-1}^2 then the distribution is not uniformly distributed with respect to intensity and suggests that the location of the blinkers is dependent on brightness of emission.

Table V. The likelihood ratio statistic and corresponding χ_{k-1}^2 values calculated from a test to determine whether active-region O V $n_\lambda = 5$, $n_p = 3$ blinkers are uniformly distributed with respect to intensity.

Wavelength	k	χ_{k-1}^2	Likelihood ratio statistic
HeI	7	24.10	2911.26
OIII	8	26.02	5132.24
OIV	9	27.87	5809.47
MgIX	6	22.11	1431.46
MgX	6	22.11	3114.04

The results from these tests are shown in Table V for the $n_\lambda = 5$, $n_p = 3$ blinkers. The blinkers are clearly not uniformly distributed with respect to the intensity of the pixels - the likelihood ratio statistic is between 65 and 210 times greater than the expected χ^2 statistic. We can investigate their distribution still further by comparing histograms

of the intensity of both the blinker pixels at the peak of the blinker and of all pixels (Figure 5). This figure shows that for all wavelengths the blinker pixels are distributed such that they are not associated with low intensity pixels. This suggests that the blinkers are preferentially located over regions of strong emission for all wavelengths including coronal ones. This result is slightly different than that for the QS blinkers which do not seem to be associated with strong coronal emission. This discrepancy between the AR and QS blinkers may be due to the stronger emission in the coronal lines in active regions.

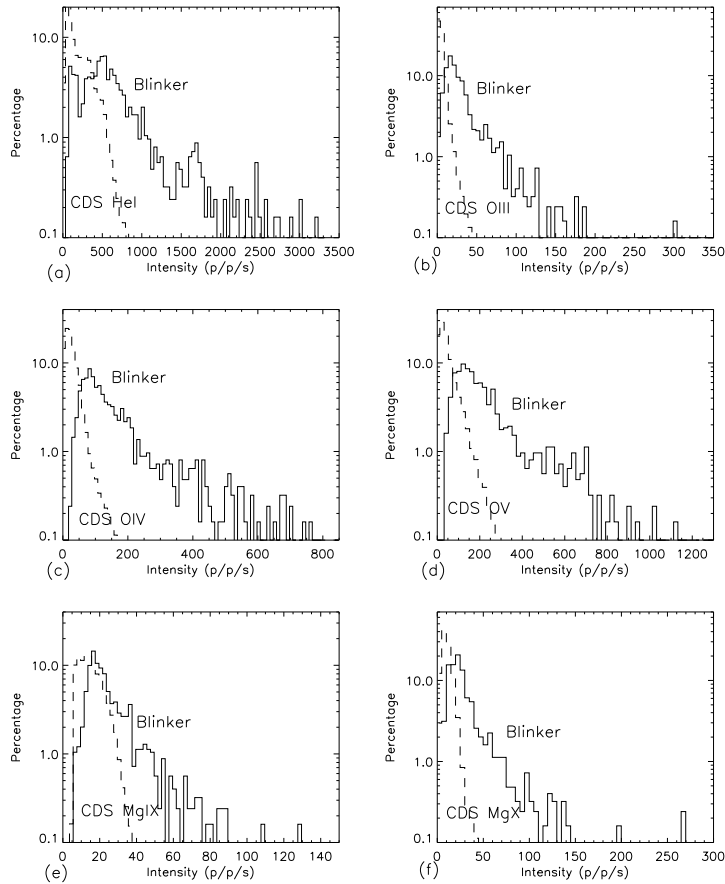


Figure 5. Histograms showing the distribution of intensity in the whole data set (dashed) and in the blinkers (solid) for (a) He I, (b) O III, (c) O IV, (d) O V, (e) Mg IX and (f) Mg X lines, respectively.

3.5. RELATIONSHIP TO THE MAGNETIC FIELD

The magnetic field plays a key role in most events in the Sun's atmosphere and blinkers are unlikely to be an exception. We, therefore, consider what magnetic fragments lie below the blinkers.

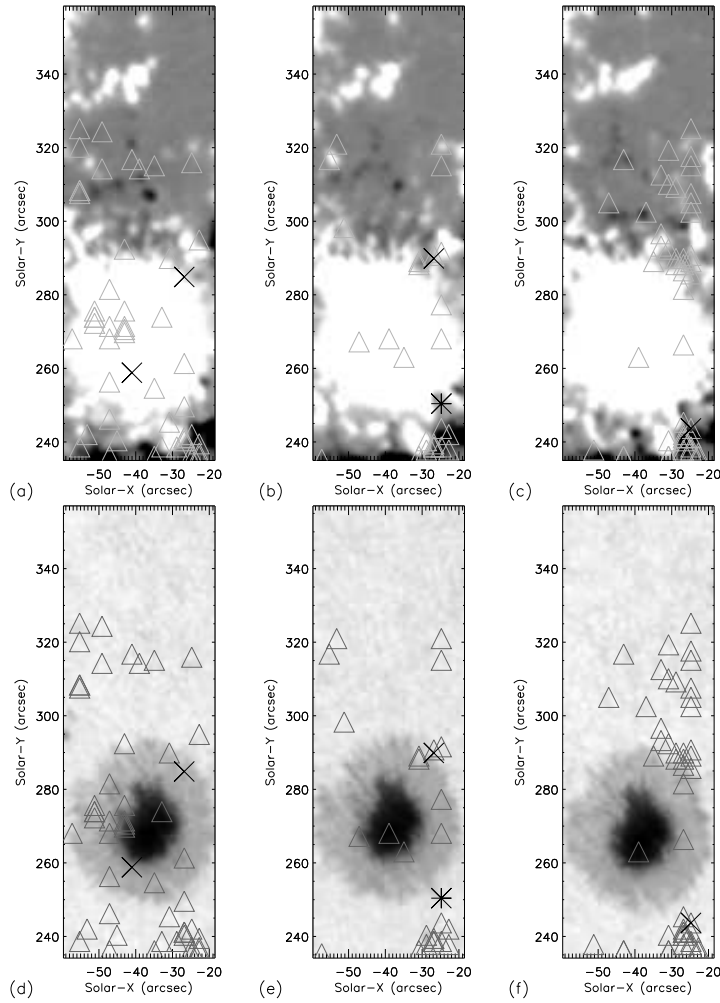


Figure 6. Comparison of the location of the midpoints of the O V $n_\lambda = 5$ and $n_p = 3$ blinkers (Δ) with the underlying magnetic field (a-c) and white light images (d-f). The sections of MDI magnetograms, with maximum colour intensity limits set for absolute fields of 500 Mx cm^2 , and MDI white light images are shown at times 20:07 (left), 22:10 (middle) and 00:07 (right). The \times s indicate the blinkers that peak in the corresponding frame and the $*$ indicates the blinker which has been discussed in detail throughout this paper.

In Figure 6 the Δ s indicate the locations of the midpoints of the $n_\lambda = 5$ and $n_p = 3$ blinkers with respect to the magnetic field and

white light images. (Note: the size of the blinkers is larger than the symbols shown). The Δ s plotted are those that occur (from left to right) in the first 1 hour 50 minutes, the next 2 hours 2 minutes and the last 1 hour and 47 minutes, respectively, of the observing sequence. The blinker shown in Figure 2d is identified with a * and is drawn over the MDI image taken at 22:10, the nearest frame to the peak of the blinker. The \times s shown on the magnetograms and white light frames indicate the blinkers that peak at the times of the MDI images underneath them. From left to right over each magnetogram and white light image there are, respectively, 51, 27 and 47 blinkers. It important to note that the underlying magnetic field can change substantially in between the frames such that the positions of the blinkers shown by the Δ s may be misleading since these blinkers do not peak at the time of the MDI image they are plotted over.

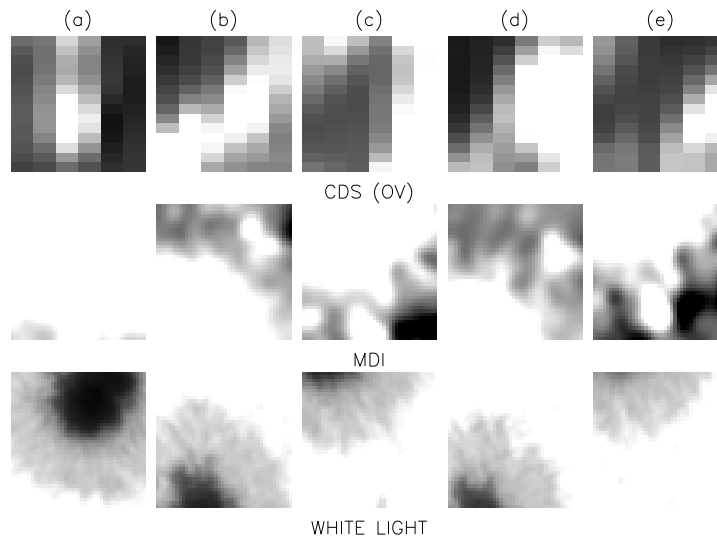


Figure 7. CDS O V images of the five blinkers indicated in Figure 6 by \times s and a *; (a-e) corresponds to their order from left to right as seen in Figure 6. The MDI magnetogram images show the magnetic field below the blinkers taken at the time of the peak of each blinker; maximum colour intensity limits are set for absolute magnetic fields above 500 Mx cm^{-2} . MDI white light images are also shown taken near to the time of the peak of each blinker.

We focus on the 5 blinkers marked with the * and \times s that peak at the times of the MDI images. Figure 7 shows a close up of each blinker as seen in O V from the CDS data, the underlying magnetic field taken by MDI and the photosphere as seen in white light. The blinkers in Figure 7 are ordered as they are seen from left to right in Figure 6. The first blinker, Figure 7a, is situated over the positive sunspot which dominates the MDI frame. From the white light it is

clear that the blinker is on the edge of the umbra and penumbra. In Figure 7b, the second blinker, which is on the edge of the penumbra of the sunspot over some smaller positive fragments, is shown. The third blinker, Figure 7c, is positioned near the edge of the sunspot in the bottom right-hand corner of the frame outside the penumbra. This blinker is found to be associated with a negative fragment rather than with the sunspot. The fourth blinker, Figure 7d, is similarly placed just outside the penumbra but this time on the edge of a large positive fragment, whilst the fifth blinker, Figure 7e, is associated with a region that includes both large positive and negative polarities, but is primarily situated over a negative fragment.

These results suggests that the nature of the magnetic fragments below blinkers does not have a unique configuration, indeed all combinations of magnetic fragments can exist below a blinker. Furthermore, it seems clear, from the blinkers located above the sunspot, that mixed polarity is not a necessary condition for a blinker to occur.

Table VI. Numbers and polarities of magnetic fragments below the $n_\lambda = 5$ and $n_p = 3$ active-region blinkers.

Polarity	Number (Size - in MDI pixels) of Magnetic Fragments		
	One (> 10)	Two: one (> 10) of major sign one (< 10) of opposite sign	One (< 10)
P	47	10	1
N	14	15	-
P+N	37	-	1

From Figure 6, it appears that there are blinkers that occur in regions where there is little or no significant magnetic fragments. This may, of course, be because the fragments associated with these blinkers have either cancelled or not yet emerged in the particular frame shown. Therefore, a crude analysis is used to investigate the types of magnetic fragments that lie below the AR blinkers. This analysis involves counting the numbers of MDI pixels with field strengths below -25 Mx cm^{-2} or above 25 Mx cm^{-2} . If there are less than 10 such pixels of one polarity below the blinker then we count that as indicating a small magnetic fragment. If, however, there are more than 10 such pixels of the same polarity with more than this field strength then we say there is a large fragment below the blinker. Table VI shows the results of the numbers and polarities of fragments below the $n_\lambda=5$ and $n_p=3$ blinkers. The results show that most (98%) blinkers occur above large

fragments of one or both polarities, and that 69% occur above regions where one polarity dominates. Furthermore, 25% occur directly above a large positive sunspot. Of these sunspot blinkers, 25% occur over the umbra and 75% above the penumbra.

3.6. COMPARISON OF THE BLINKERS IN SUNSPOT AND NON-SUNSPOT REGIONS

Table VII. Properties of the active-region O V $n_\lambda = 5$, $n_p = 3$ blinkers that were observed above the sunspot in either the umbra or penumbra, non-sunspot regions and the whole active region.

Properties	Sunspot		Non-Sunspot	Active Region
	Umbra	Penumbra		
No. of blinkers	6	18	101	125
Global frequency (s^{-1})	12.5	10.8	14.4	13.7
Mean intensity enhancement factor	2.0	2.4	2.4	2.4
Mean area ($\times 10^7$ km ²)	3.2	5.2	3.8	3.9
Mean lifetime (minutes)	19.6	17.0	17.5	17.5
Mean rise time (minutes)	11.7	8.1	8.5	8.6
Mean fall time (minutes)	7.8	8.9	9.0	8.9
Rise time > Fall time	4	6	44	54
Rise time < Fall time	1	10	37	48
Rise time \approx Fall time	1	2	20	23

As seen in Section 3.5, the AR O V blinkers identified are found both inside a sunspot with their midpoints situated above both the umbra and penumbra, as well as in the surrounding (non-sunspot) region. To check that these types of events are all the same we compare their properties which are shown in Table VII. Most of the properties of the three types of blinker are fairly similar. There are a few small differences, but due to the low statistics it is not clear whether these are significant. For instance, the mean lifetimes of the umbral, penumbral and non-sunspot blinkers appear to be approximately the same, although the umbral blinkers seem to last a little (11%) longer and the penumbral blinkers seem to last a little (3%) shorter than the non-sunspot blinkers. The mean areas of the umbral and penumbral blinkers are 16% smaller and 37% larger, respectively, than those for the non-sunspot blinkers, however, these differences are still within the observed

spread of non-sunspot blinker areas. The penumbral blinkers appear to have the same mean intensity enhancement factor as non-sunspot blinkers, however, the umbral ones are 17% weaker. The frequency of occurrence of sunspot blinkers in both the umbra and penumbra is slightly lower than that for non-sunspot blinkers, but is still higher than that for QS blinkers. There are more umbral blinkers with rise times greater than fall times and more penumbral blinkers with rise times less than fall times than in the non-sunspot case, however, this is most likely to be due to the small numbers of events detected. We therefore conclude that the properties of the three different types of blinkers are similar enough to suggest that sunspot blinkers are essentially the same as non-sunspot blinkers. Finally though, we note that only 46% of the O V sunspot blinkers can also be observed in either He I or O IV, whereas 73% and 91%, respectively, of the non-sunspot O V blinkers can also be observed in these lines. The physical significance of this discrepancy is not clear. Indeed, it may again be simply be due to the small number of sunspot blinkers observed.

4. Conclusions

We have identified events in an active region that have the same characteristics as QS blinkers (Paper 1) and have named these events ‘active-region blinkers’. Two similar events had previously been found by Walsh et al. (1997), but little was known about these events in general. We have found that AR blinkers have mean lifetimes between 16.5 and 19.3 minutes, mean areas between 2.4×10^7 and 4.3×10^7 km² and mean intensity enhancement factors between 1.8 and 3.3. They are more abundant than QS blinkers and have a global frequency between 7 and 28 s⁻¹. These characteristics suggest that AR blinkers are a little larger and slightly more intense than QS blinkers, but have approximately the same lifetimes. Furthermore, our results suggest that, like QS blinkers, AR blinkers are enhancements in density or filling factor and are not temperature events.

In all wavelengths the light curves of the blinkers are very similar. Indeed, approximately 5-10% of the AR blinkers show peaks in both the coronal lines (Mg IX and Mg X) that are significant enough to count as blinkers. The presence of these coronal blinkers is the most significant difference between AR and QS blinkers. It is possible that these signatures are only visible because the counts in the coronal lines are much higher in an active region than in the quiet Sun. Even if the peaks in the coronal lines are not significant enough to be blinkers they are still indicating that an event has occurred. The coronal signatures

of blinkers are very similar to those found in nanoflares (i.e. peaks in intensity) and, therefore, if the coronal events we observe with peak factors greater than 3 are actually nanoflares our results suggest that at least 15% of active-region blinkers could be associated with small nanoflares. This possible association is rather strange since nanoflares are believed to be heating events (Krucker and Benz, 1998; Parnell and Jupp, 2000; Aschwanden et al., 2000a; Aschwanden et al., 2000b) and yet we have found from line ratios that O V blinkers are not temperature enhancements. Clearly, before any firm conclusions about the connection between nanoflares and blinkers can be reached a proper investigation comparing CDS and TRACE or EIT images needs to be made.

We have shown that blinkers are located over the regions with the strongest emission from all lines, chromospheric, transition and coronal. This suggests that blinkers occur above sites of active-region network and plage regions.

Our analysis of the magnetic field below blinkers reveals that blinkers can occur both inside a sunspot and in the surrounding non-sunspot region. The blinkers that occur inside a sunspot occur both in the umbra and the penumbra. Furthermore, the properties of the blinkers in these regions are comparable and so we believe that they are both created by the same mechanism. Investigations of the magnetic fragments below blinkers show that no specific magnetic fragment pattern is needed for blinkers to occur. However, blinkers do show a preference for regions of strong unipolar field.

From the results presented here for AR blinkers and in Paper 1 for QS blinkers it appears as if the quiet-Sun, non-sunspot and sunspot blinkers are all effectively the same sorts of event and, hence, they are all created by the same mechanism. Let us consider briefly what this mechanism might be.

Blinkers generally do not occur above regions of mixed polarity field and so reconnection in the form suggested to power bright points and nanoflares (e.g., Priest et al., 1994, Parnell et al., 1994, and Longcope et al., 2001) is unlikely to be responsible for these events. In Paper 1, several possible mechanisms were suggested and these are listed below.

- Iso-thermal compression of pre-existing plasma along field lines.
- Gathering together of field lines with pre-existing plasma at transition region temperatures to increase filling factor.
- Distant reconnection of field lines causing them to be ‘slung-shot’ over.

In light of our results for AR blinkers creating the blinkers by isothermal compression is still a possibility, since this could occur in a unipolar magnetic field. The gathering of magnetic field lines is still also a possible mechanism since inside a sunspot the magnetic field is continually being squeezed and buffeted by the convection motions below, however, it is uncertain how such motions at the surface would effect the field above. It is more likely that any squeezing of the field must occur in the transition region itself. However, the idea of distant reconnection is less likely since, although the field lines that extend out from a sunspot will undoubtedly have distant connections in, say, another sunspot and these field lines may well reconnect, the field lines in the sunspot will always be predominantly vertical and are therefore unlikely to be ‘slung-shot’ over. Hence, changes due to line-of-sight effects are unlikely.

Several further ideas suggested in Priest et al. (2001) were also discussed in Paper 1. The increased global birth rate of AR blinkers is still too small to account for the suggestion that blinkers are connected with the compression by spicules. Furthermore, the suggestion that blinkers are cool, short, low-lying loops does not fit with our observations of blinkers in a large sunspot where such field lines are unlikely to occur. Another suggestion is that blinkers are at the base of hot coronal loops. Comparison of CDS data with TRACE or SXT data showing hotter coronal lines would enable us to determine whether blinkers do actually occur near the base of hot loops and produce a ‘blinking effect’. Furthermore, high resolution images would give a better idea of the coronal structures above the blinkers, and would, indeed, show if blinkers even had signatures at these hotter temperatures.

The two final mechanisms suggested by Priest et al. (2001) were that blinkers are connected with heating and evaporating plasma or with cooling and draining plasma. This is a possibility since the cadence of the data analysed is not sufficient to detect any time delay between blinkers in different wavelengths. However, so far, no substantial flows have been seen in blinkers (Parnell et al., 2001) and no consensus has been reached on the typical direction of flows in blinkers, thus we cannot verify either way whether these mechanisms are likely candidates.

Other phenomena have been identified in the transition region above active regions. These include active transition-region brightenings as described by Mason et al. (1997) and Fludra et al. (1997). Mason et al. (1997) describe events observed in the Mg V (353 Å) and Mg VI (349 Å) emission lines (formed at the transition region temperatures 3×10^5 K and 4×10^5 K) that showed no significant enhancement in the hotter Mg IX and Mg X coronal lines. Fludra et al. (1997) also observed bright compact sources in transition region lines using CDS. They found

events with a lifetime of at least 12 hours near regions of strong magnetic flux, such as near a sunspot and over lying the penumbra or the umbra. Clearly, since the lifetimes of the AR blinkers are 30-40 times shorter than those of the active transition-region brightenings, they are not the same events, however, it is possible that several blinkers could occur in one active transition-region brightening. Analysis of a data set including O IV (554 Å), O V (629 Å), Mg V (353 Å) and Mg VI (349 Å) would need to be undertaken to establish whether these events are connected.

Events in the corona that may be connected to AR blinkers are nanoflares, microflares or other small flaring events such as active-region transient brightenings (ARTBs) which were observed with Yohkoh/SXT and first described by Shimizu et al. (1994). ARTBs are observed to have temperatures of between 4–8 MK, with durations of 2–7 minutes (Shimizu, 1995). The lengths and widths of the events are given as $5 \times 10^3 - 4 \times 10^4$ km and $2 \times 10^3 - 7 \times 10^3$ km, respectively, giving a range of areas between $1 \times 10^7 - 2.8 \times 10^8$ km². The energy released from these events is estimated by Shimizu et al. (1994) to be approximately 10^{29} ergs, suggesting that the ARTBs are at the low end of the sub-flare energy range, but larger than micro-flares. The global frequency of these events was found to be approximately 3 per minute in *active* active regions and 1 per hour in *quiet* active regions (Shimizu et al., 1994). Furthermore, Berghmans & Clette (1999) claim to have detected the ‘cooler and weaker EUV counterparts’ of the ARTBs described by Shimizu (1995) using EIT/SOHO Fe XII (formed at 1.6×10^6 K) data. These events have durations of between 1.5 – 10 minutes, and areas between $1.5 - 10 \times 10^7$ km². They suggest that the elongated nature of these events means that they may be related to compact loops. They also suggest that the average intensity enhancement of 100% (i.e. a factor of 2) is quite exceptional. More recently, Berghmans et al. (2001) analysed SXT, EIT and TRACE data for ARTBs. They find that the stronger ARTBs (found using SXT) correspond to several EUV brightenings, but the weaker events have no EUV counterpart at all. Similarly the weaker EUV events have no soft X-ray counterpart.

AR blinkers and ARTBs appear to be of a similar size, however, ARTBs tend to have shorter lifetimes than AR blinkers. It is possible that this difference may be due to the low time resolution of 2.5 minutes of our data meaning that the shortest blinker lifetime that we can observe is just 5 minutes. However, the average lifetime of the blinkers is 17 minutes with only a few ($\approx 7\%$) of blinkers having lifetime less than 10 minutes and so the difference in lifetime is unlikely to be due to temporal resolution effects. Clearly, since we have only looked at a small section of an active region it is difficult to compare frequencies

of events, however, it is likely that the rate of blinker occurrence is somewhere in between 3 per minute and 1 per hour and so comparable with the frequency of ARTBs. Furthermore, ARTBs are not generally seen inside sunspots, but more around their edges or in plage regions, unlike AR blinkers. Since we have not calculated the energy of our blinkers it is hard to compare blinker energies with those of ARTBs, however Walsh et al. (1997) indicate that one of the AR blinkers they found had energies of just 3×10^{27} ergs in He I, 3×10^{25} ergs in O V, 2×10^{24} ergs in Mg IX and 3×10^{24} ergs in Fe XVI. These energies are probably at the small end of the spectrum of energies estimated for ARTBs and no conclusions can be formed from a single event. From the GOES data it is possible to see that there were just 3 flares during our observing period, 2 of which were GOES B2 level and one of which was GOES B9. From the data it is not possible to say where the largest of the GOES flares originated, however, the other two flares were seen over AR 8243 which is the active region we observed. This suggests that the ARTB activity may have been fairly low, whereas we see quite a few AR blinkers. Furthermore, AR blinkers are thought to be density or filling factor enhancements whereas ARTBs are temperature events. It is therefore hard to say whether there is a relation between AR blinkers and either ARTBs or their EUV counterparts and this possibility needs testing.

Acknowledgements

CDS was built and is operated by a consortium led by the Rutherford Appleton Laboratory and including the Mullard Space Science Laboratory, the NASA Goddard Space Flight Center, Oslo University and the Max-Planck-Institute for Extraterrestrial Physics, Garching. MDI is a project of the Stanford-Lockheed Institute for Space Research and is a joint effort of the Solar Oscillations Investigation (SOI) of Stanford University and the Solar and Astrophysics Laboratory of the Lockheed-Martin Advanced Technology Center. SOHO is a mission of international cooperation between ESA and NASA. CEP and DB would like to thank Dave Pike, Peter Jupp and David Berghmans for their help and useful comments. CEP would like to thank the Royal Astronomical Society for support as the RAS Sir Norman Lockyer Fellow. DB acknowledges support from the Particle Physics and Astronomy Research Council.

References

- Aschwanden, M.J., Nightingale, R.W., Tarbell, T.D., Wolfson, C.J.: 2000, *Astrophys. J.* **535**, 1027.
- Aschwanden, M.J., Tarbell, T.D., Nightingale, R.W., Schrijver, C.J., Title, A., Kankelborg, C.C., Martens, P. and Warren, H.P.: 2000, *Astrophys. J.* **535**, 1047.
- Athay, R.G.: 1984, *Solar Phys.* **93**, 123.
- Athay, R.G., White, O.R., Lites, B.W. and Bruner, E.C., Jr.: 1980, *Solar Phys.* **66**, 357.
- Berghmans, D. and Clette, F.: 1999, *Solar Phys.* **186**, 207.
- Berghmans, D., Clette, F. and Moses, D.: 1998, *Astron. Astrophys.* **336**, 1039.
- Berghmans, D., McKenzie, D. and Clette, F.: 2001, *Astron. Astrophys.* **369**, 291.
- Bewsher, D., Parnell, C.E. and Harrison, R.A.: 2001, *Solar Phys.*, in press.
- Bewsher, D., Parnell, C.E. and Pike, C.D.: 2002, in preparation.
- Brković, A., Solanki, S.K. and Rüedi, I.: 2001, *Astron. Astrophys.* **373**, 1056.
- Bruner, E.G., Jr. and Lites, B.W.: 1979, *Astrophys. J.* **228**, 322.
- Dere, K.P., Bartoe, J.D.F., Brueckner, G.E., Dykton, M.D., and van Hoosier, M.E.: 1981, *Astrophys. J.* **249**, 333.
- Fludra, A., Brekke, P., Harrison, R.A., Mason, H.E., Pike, C.D., Thompson, W.T. and Young, P.T.: 1997, *Solar Phys.* **175**, 487.
- Habbal, S.R., Withbroe, G.L. and Ronan, R.: 1985, *Solar Phys.* **98**, 323.
- Harrison, R.A.: 1997, *Solar Phys.* **175**, 467.
- Harrison, R.A., Fludra, A., Pike, C.D., Payne, J., Thompson, W.T., Poland, A.I., Breeveld, A.A., Culhane, J.L., Kjeldseth-Moe, O., Huber, M.C.E. and Aschenbach, A.: 1995, *Solar Phys.* **162**, 223.
- Harrison, R.A., Lang, J., Brooks, D.H. and Innes, D.E.: 1999, *Astron. Astrophys.* **351**, 1115.
- Krucker, S. and Benz, A.O.: 1998, *Astrophys. J.* **501**, L213.
- Lites, B.W. and Hansen, E.R.: 1977, *Solar Phys.* **55**, 347.
- Longcope, D.W., Kankelborg, C.C., Nelson, J.L. and Pevtsov, A.A.: 2001, *Astrophys. J.* **553**, 429.
- Mason, H.E., Young, P.R., Pike, C.D., Harrison, R.A., Fludra, A., Bromage, B.J.I. and Del Zanna, G.: 1997, *Solar Phys.* **170**, 143.
- Parnell, C.E., Bewsher, D., Harrison, R.A. and Hood, A.W.: 2001, *Recent Insights into the Physics of the Sun and Heliosphere: Highlights from SOHO and other Space Missions, International Astronomical Union. Symposium no. 203. ASP Conference Series (ed P. Brekke, B. Fleck and J. Gurman)*, 359-361.
- Parnell, C.E. and Jupp, P.E.: 2000, *Astrophys. J.* **529**, 554.
- Parnell, C.E., Priest, E.R. and Titov, V.S.: 1994, *Solar Phys.* **153**, 217.
- Porter, J.G., Toomre, J., and Gebbie, K.B.: 1984, *Astrophys. J.* **283**, 879.
- Priest, E.R., Hood, A.W. and Bewsher, D.: 2001, *Solar Phys.*, in press.
- Priest, E.R., Parnell, C.E. and Martin, S.F.: 1994, *Astrophys. J.* **427**, 459.
- Scherrer, P.H., Bogart, R.S., Bush, R.I., Hoeksema, J.T., Kosovichev, A.G., Schou, J., Rosenberg, W., Springer, L., Tarbell, T.D., Title, A., Wolfson, C.J. and Zayer, I., MDI Engineering Team.: 1995, *Solar Phys.* **162**, 129.
- Shimizu, T.: 1995, *Publ. Astron. Soc. Japan* **47**, 251.
- Shimizu, T., Tsuneta, S., Acton, L.W., Lemen, J.R. and Uchida, Y.: 1994 *Publ. Astron. Soc. Japan* **44**, L147.
- Walsh, R.W., Ireland, J., Harrison, R.A. and Priest, E.R.: 1997, *Proceedings of the Fifth SOHO Workshop, 'The Corona and Solar Wind near Minimum Activity'*. *ESA SP-404*, 717.

Withbroe, G.L., Habbal, S.R. and Ronan, R.: 1985, *Solar Phys.* **95**, 297.

